Brief Communication

JCBFM

Journal of Cerebral Blood Flow & Metabolism
2016, Vol. 36(4) 702–708

DOI: 10.1177/0271678X15627657
jcbfm.sagepub.com
SAGE

Imaging the role of toll-like receptor 4 on cell proliferation and inflammation after cerebral ischemia by positron emission tomography

Ana Moraga[1], Vanessa Gómez-Vallejo[2], María Isabel Cuartero[1], Boguslaw Szczupak[3], Eneko San Sebastián[3], Irati Markuerkiaga[3], Jesús M Pradillo[1], Makoto Higuchi[4], Jordi Llop[2], María Ángeles Moro[1], Abraham Martín[3] and Ignacio Lizasoain[1]

Abstract

The influence of toll-like receptor 4 on neurogenesis and inflammation has been scarcely explored so far by using neuroimaging techniques. For this purpose, we performed magnetic resonance imaging and positron emission tomography with 3′-deoxy-3′-[^{18}F]fluorothymidine and [^{11}C]PK11195 at 2, 7, and 14 days following cerebral ischemia in TLR4$^{+/+}$ and TLR4$^{-/-}$ mice. MRI showed similar infarction volumes in both groups. Despite this, positron emission tomography with 3′-deoxy-3′-[^{18}F]fluorothymidine and [^{11}C]PK11195 evidenced an increase of neurogenesis and a decrease of inflammation in TLR4$^{-/-}$ mice after ischemia. These results evidence the versatility of neuroimaging techniques to monitor the role of toll-like receptor 4 after cerebral ischemia.

Keywords

Positron emission tomography, magnetic resonance imaging, middle cerebral artery occlusion, cerebral ischemia, toll-like receptor 4, 3′-deoxy-3′-[^{18}F]fluorothymidine, [^{11}C]PK11195, T_2W-MRI

Received 10 August 2015; Revised 20 December 2015; Accepted 21 December 2015

Introduction

Focal cerebral ischemia triggers different cellular responses that occur the following days after the onset of ischemia. These events include both neuroinflammation and regenerative responses that involve activation of resident microglia/macrophages and the proliferation of endogenous neural stem cells.[1,2] Innate immunity through toll-like receptors induces and mediates an inflammatory response by production of pro-inflammatory mediators[3] that are involved in the brain damage produced by ischemia. Indeed, we and others demonstrated the implication of toll-like receptor 4 (TLR4) in the acute cerebral damage and inflammation elicited by an ischaemic injury.[4–7] TLR4 is predominantly expressed in microglia; importantly, it has been described that activated microglia is not always detrimental on stroke outcome but can mediate repair effects.[8] In this context, inflammation involves a dramatic increase in the expression of the translocator protein (18 kDa) (TSPO).[9] For this reason, these receptors have become a potential target to study the

[1]Unidad de Investigación Neurovascular, Departamento de Farmacología, Facultad de Medicina, Universidad Complutense de Madrid and Instituto de Investigación Hospital 12 de Octubre (i + 12), Madrid, Spain
[2]Radiochemistry, Molecular Imaging Unit, CIC, biomaGUNE, San Sebastian, Guipuzcoa, Spain
[3]Molecular Imaging Unit, CIC biomaGUNE, San Sebastian, Guipuzcoa. Spain
[4]Molecular Imaging Center, National Institute of Radiological Sciences, Chiba, Japan

Corresponding authors:
Abraham Martín, Unidad de Imagen molecular; CICbiomaGUNE, Edificio Empresarial "C," P° Miramon 182, 2009, San Sebastian, Guipuzcoa, Spain.
Email: amartin@cicbiomagune.es and
Ignacio Lizasoain, Unidad de Investigación Neurovascular. Departamento de Farmacología, Facultad de Medicina. Universidad Complutense de Madrid. 28040, Madrid, Spain.
Email: ignacio.lizasoain@med.ucm.es

neuroinflammatory processes following brain injury using positron emission tomography (PET) imaging.[10] Specifically, [^{11}C]PK11195 is a selective radioligand that has been widely used to evaluate TSPO expression in rodents[11,12] and in the human brain[13] after cerebral ischemia. On the other hand, TLR4 plays an important role in adult neurogenesis by inhibiting both neuronal proliferation and differentiation in rat under physiological conditions.[14] Of note, we have demonstrated that TLR4 modulates stroke-induced neurogenesis by promoting neuroblasts migration and thus increasing the number of new cortical neurons after stroke.[15] Likewise, cell proliferation in rat brain after cerebral ischemia may be visualized in vivo with PET using the 3′-deoxy-3′-[^{18}F]fluorothymidine ([^{18}F]FLT).[1] Therefore, the purpose of the present study was to image cell proliferation and inflammation as TSPO receptor expression by using PET with [^{18}F]FLT and [^{11}C]PK11195, respectively, in the presence and the absence of TLR4 following experimental stroke in mice.

Materials and methods

Animals and surgery

Adult male C57BL/10ScNJ (TLR4$^{-/-}$) (n = 21) and C57BL/10 J (TLR4$^{+/+}$) (n = 26) (2–3 months old) were used (Jackson Labs, Bar Harbor, ME). Animal studies were approved by the animal ethics committee of CIC biomaGUNE and local authorities and were conducted in accordance with the ARRIVE guidelines and Directives of the European Union on animal ethics and welfare. Since we demonstrated that TLR4$^{+/+}$ mice showed bigger infarcts than TLR4$^{-/-}$ mice[4] and that cell proliferation is dependent on infarct size after stroke,[15] we performed a proximal occlusion of the middle cerebral artery (MCAO) in TLR4$^{-/-}$ mice (n = 16) and a distal occlusion of the MCAO in TLR4$^{+/+}$ mice (n = 13) to obtain similar infarct sizes and thus to avoid the bias due to different infarct sizes. Briefly, permanent focal cerebral ischemia was done under anesthesia with 2% isofluorane in 100% O_2 by ligature of the MCA before its bifurcation between the frontal and parietal branches (proximal occlusion) or more distally (distal occlusion) as described elsewhere.[15] Sham operation (n = 10) and nonoperated (n = 8) mice were also included in the study as controls.

Magnetic resonance imaging (MRI) and infarct determination

MRI experiments were performed to examine the extent of brain infarction in those animals included in the nuclear studies. T_2-weighted (T_2W) MRI scans were performed in ischemic animals (n = 13) at 24 h after occlusion. Measurements were performed under 1.5–2% of isofluorane in 100% O_2 and normothermic conditions by using an 11.7 T Bruker Biospec system with a 72 mm volumetric quadrature coil for excitation and a 20 mm surface coil for reception. Acquisition parameters for the T2 weighted spin echo images were as follows: TR/TE = 5000/12 ms, fov = 18×18 mm^2, matrix = 200×200, averages = 4, slice thickness = 0.5 mm and n° slices = 32. T_2W images were used to manually define the percent of hemisphere infarcted volume (HIV %) using ImageJ 1.441 (NIH, Bethesda, MD, USA) and the following formula: HIV% = [1 − (*L*N/R)] × 100.

Radiochemistry

[^{11}C]PK11195 was synthesized by methylation (R)-*N*-desmethyl-PK11195 (1 mg, ABX) using [^{11}C]CH_3I prepared by the gas phase method.[16] Methylation was conducted following the captive solvent method[17] using dimethylsulfoxide as the solvent and potassium hydroxide as the base. Purification by high-performance liquid chromatography (HPLC) (stationary phase: Mediterranean Sea18, 9.6 mm × 250 mm, 5 µm particle size, Teknokroma, Spain; mobile phase: water/acetonitrile, 25/75; retention time: 7–8 min) followed by reformulation and sterile filtration yielded [^{11}C]PK11195 with average decay corrected radiochemical yield and specific activity of 40 ± 8% and 125 ± 38 GBq/µmol, respectively, in an overall production time of 42 min. Radiochemical purity was higher than 99% at injection time.

The synthesis of 3′-deoxy-3′-[^{18}F]fluorothymidine ([^{18}F]FLT) was performed as described earlier[18] using a TRACERlab FX_{FN} synthesis module (GE Healthcare). After purification by HPLC (stationary phase: VP125/10 Nucleosil 100-7 C18 column, Macherey-Nagel; mobile phase: 0.01 M aqueous NaH_2PO_4/ethanol, 90/10; retention time: 13–14 min) and sterile filtration, injectable [^{18}F]FLT solution was obtained with nondecay corrected radiochemical yield of 7.5 ± 1.1% in an overall production time of 62 min. Radiochemical purity was above 95% in all cases.

PET scans and data acquisition

PET scans were repeatedly performed in ischemic TLR4$^{-/-}$ (n = 8) and TLR4$^{+/+}$ (n = 5), sham-operated (n = 10) at two, seven, and 14 days after surgery as well as in nonoperated rats used as controls (n = 8) using a GE eXplore Vista CT camera. Animals were subjected to two PET scans with [^{11}C]PK11195 and [^{18}F]FLT. First, mice were anesthetized, injected with around 20 MBq of [^{11}C]PK11195 and placed into the PET camera under 1.5–2% of isofluorane in 100% O_2 and

normothermic conditions. Brain dynamic images were acquired for 10 frames and 27 min. Second, after at least 180 min, animals were reanesthetized, injected with around 20 MBq of [^{18}F]FLT and scanned with PET for 18 frames and 60 min. After PET scans, CT acquisitions were performed providing anatomical information and the attenuation map for image reconstruction. Dynamic acquisitions were reconstructed with filtered back projection using a Ramp filter with a cutoff frequency of 0.5 mm^{-1}.

PET images were analyzed using PMOD image analysis software (PMOD Technologies Ltd, Zürich, Switzerland). For the analysis of PET signal, both PET images and an MRI (T_2W) mouse brain template were separately coregistered to the CT of the same animal to generate a spatial normalization. Subsequently, MRI brain template was coregistered to PET images. Two types of volumes of interest (VOIs) were established as follows: (i) For the [^{11}C]PK11195, a first set of VOIs was automatically generated in the ipsilateral brain cortex by using the region proposed by the PMOD mouse brain template. (ii) For the [^{18}F]FLT, a second set of spherical VOIs was manually defined in the ipsilateral subventricular zone. For quantification of both VOIs, last three frames (last 15 min of PET acquisition for [^{18}F]FLT and 10 min for [^{11}C]PK11195) were averaged and the uptake in each VOI (mean ± standard deviation) was determined and expressed as percentage of injected dose per cubic centimeter (%ID/cc).

Brain dissociation and BrdU cell suspensions analysis by flow cytometry

Flow cytometry was performed at 48 h after MCAO in TLR4$^{-/-}$ (n = 4) and TLR4$^{+/+}$ (n = 5). Mice brain were removed, ipsilateral and contralateral cortex were dissected with a scalpel, placed into 15 ml of ice-cold HBSS, and dissociated in a single cell suspension using a Potter-Elvehjem-type tissue grinder with teflon pestles. Cell suspension was filtered on 70 µm nylon mesh strainers and centrifuged at 300 g for 10 min. Pellets were resuspended in 35% Percoll isotonic. Cells were centrifuged at 800 g for 45 min at 4°C and pelleted cells were fixed and permeabilized. After DNAse treatment, cells were incubated whit an anti-BrdU antibody and 500,000 cells were acquired using a FACSCalibur flow cytometer with CellQuest software (BD Pharmingen, San Jose, CA). Isotype controls (Miltenyi) and BrdU negative controls were used in parallel. Data were analyzed with FlowJo software (Tree Star Inc, USA).

Immunohistochemistry and cell counts

Immunohistochemistry staining was performed at day 2 after ischemia. TLR4$^{-/-}$ (n = 4) and TLR4$^{+/+}$ (n = 3) mice were terminally anesthetized followed by transcardiac perfusion through the left ventricle with 0.1 M phosphate buffer as a vascular rinse, followed by a fixing solution containing 4% paraformaldehyde in 0.1 M phosphate buffer (pH 7.4). Brains were removed, postfixed overnight, and placed in 30% sucrose for 48 h. Coronal series sections (40 µm) were cut on a freezing microtome (Leica SM2000R; Leica Microsystems GMbH, Wetzlar, Germany) and stored in cryoprotective solution. Double-label immunofluorescence was performed on free-floating sections and incubated overnight at 4°C with the primary antibodies rabbit anti-mouse TSPO (NP155, 1:1000) and rat anti-mouse CD11b (1:300; AbD Serotec, Raleigh, NC, USA). After incubating with the primary antibody, sections were washed, incubated for 2 h with secondary antibodies Alexa Fluor 488 goat anti-rabbit IgG and Alexa Fluor 594 goat anti-rat (ThermoFisher, Madrid, Spain), and mounted with a prolong antifade kit in slices (ThermoFisher, Madrid, Spain). Images acquisition was performed with an Axio Observer Z1 (Zeiss, Madrid, Spain) equipped with a motorized stage. The number of TSPO/CD11b-immunopositive cells within the ischemic area was assessed at day 2 after ischemia. Cells were counted in 10 different fields at 100X magnification. Representative images of areas showing the highest staining density was analyzed using ImageJ version 1.48v (NIH, Bethesda, MD, USA).

Statistical analysis

Data were expressed as mean ± SD. Imaging comparisons between groups were performed using unpaired Student's *t*-test and one-way ANOVA with the Dunnett's multiple comparison tests for post hoc analysis for imaging studies. Flow cytometry values were compared using two-way ANOVA with Bonferroni's post hoc test. Microglial expression of TSPO receptor at day 2 after ischemia in TLR4$^{+/+}$ and TLR4$^{-/-}$ was compared using an unpaired t-test. Differences were considered significant at $p < 0.05$. Statistical analyses were performed with GraphPad Prism version 6 software.

Results

Effect of TLR4 on SVZ cell proliferation by using [^{18}F]FLT PET

To study the effect of TLR4 on SVZ cell proliferation without the influence of lesion size as we have recently demonstrated,[15] a distal occlusion in TLR4$^{+/+}$ and a proximal occlusion in TLR4$^{-/-}$ were carried out. The extent of brain damage was assessed using T_2W-MRI at one day after ischemia onset. Both groups of mice

subjected to nuclear studies presented similar infarct volumes (Figure 1(a)). Our data evidenced that the absence of TLR4 promotes cell proliferation in the ispilateral subventricular zone (SVZ) after MCAO, as demonstrated by an increase of [^{18}F]FLT binding in the SVZ at day 2 after ischemic onset when compared with those from TLR4$^{+/+}$ mice (Figure 1(b)). TLR4$^{-/-}$ mice evidenced a significant over-increase of the [^{18}F]FLT PET signal at day 2 in relation to control (Figure 1(c), $p < 0.05$) and TLR4$^{+/+}$ mice (Figure 1(c), $p < 0.05$) that was followed by a progressive decrease over time. Likewise, the contralateral SVZ area did not evidence [^{18}F]FLT binding changes in the absence or presence of TLR4 (Figure 1(d)). Hence, these results evidenced a role of TLR4 on ischemia-induced neurogenesis in mice.

Role of TLR4 on microglia proliferation by using [^{11}C]PK11195 PET and flow cytometry

The time course of the TSPO receptor was evaluated using [^{11}C]PK11195 in both TLR4$^{+/+}$ and TLR4$^{-/-}$ mice at two, seven, and 14 days following pMCAO (Figure 2(a)). At day 2, TLR4$^{+/+}$ mice showed a significant increase in the [^{11}C]PK11195 PET signal in the ipsilateral cortical region with respect to those in ischemic TLR4$^{-/-}$ and control wild-type mice (Figure 2(b); $p < 0.05$). This was followed by a later significant signal increase in both TLR4$^{+/+}$ and TLR4$^{-/-}$ when compared to control PET data (Figure 2(b); $p < 0.05$). At day 14 after ischemia onset, [^{11}C]PK11195 signal decreased in both animal groups. Likewise, sham-operated animals did not experience TSPO changes over time evidencing the lack of effect of the surgery in the [^{11}C]PK11195 signal uptake. In the contralateral cortex, [^{11}C]PK11195 PET signal did not show significant changes in both TLR4$^{+/+}$ and TLR4$^{-/-}$ mice (Figure 2(c)). Therefore, these results evidenced TLR4-induced inflammatory response following cerebral ischemia in mice. Likewise, we have determined the number of new proliferative cells (BrdU+ cells) at cortical area by using flow cytometry. We have found that TLR4$^{+/+}$ mice show a significant increase in the BrdU positive cells (proliferative cells) in the ipsilateral cortical region with respect to those in ischemic TLR4$^{-/-}$ at two days after ischemic insult (Figure 2(d)). In the contralateral cortex, we did not find any significant changes in both TLR4$^{+/+}$ and TLR4$^{-/-}$ mice (Figure 2(d)). Finally, immunohistochemistry evidenced the expression of TSPO receptor in microglial cells in both TLR4$^{+/+}$ and TLR4$^{-/-}$ mice at day 2 after cerebral ischemia. Nevertheless, the number of TSPO^{+}/CD11b^{+} cells showed a significant increase of microglial cells expressing TSPO receptors in TLR4$^{+/+}$ in

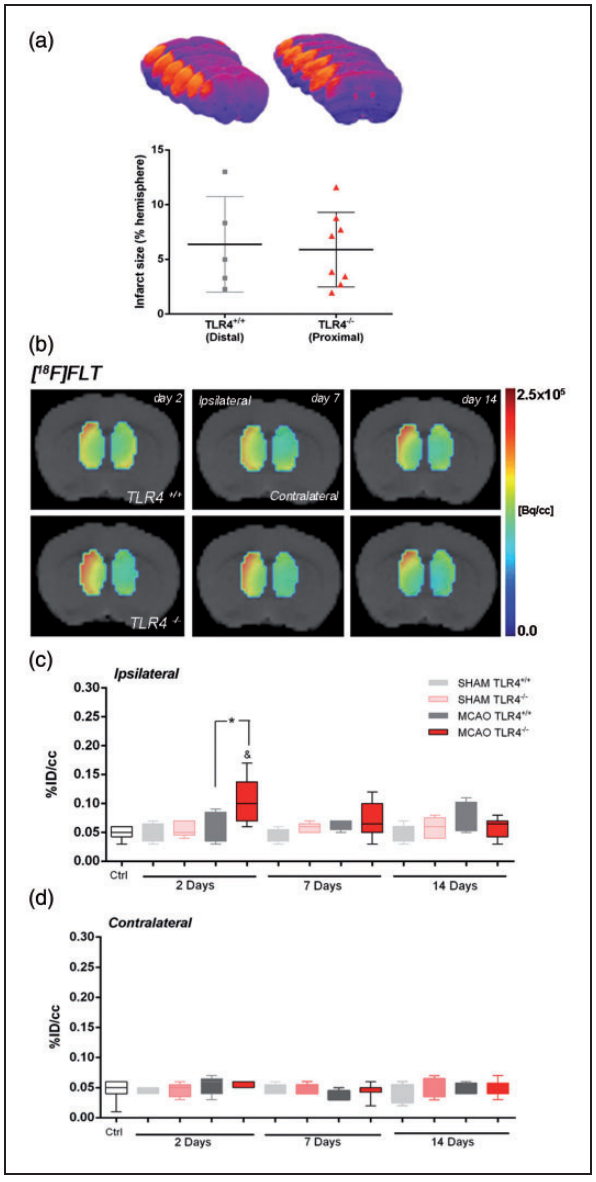

Figure 1. Effect of TLR4 on SVZ cell proliferation by using [^{18}F]FLT PET. The infarct size was determined by MRI at 24 h after MCAO in mice that express TLR4 normally (gray column; C57BL/10J mice: *TLR4*$^{+/+}$) and in TLR4-deficient mice (red column; C57BL/10ScNJ mice: *TLR4*$^{-/-}$) after distal and proximal occlusions (see "Materials and Methods" section) (a). Normalized coronal PET images of [^{18}F]FLT for TLR4$^{+/+}$ (upper row) TLR4$^{-/-}$ (lower row) at two, seven, and 14 days after cerebral ischemia are coregistered with a MRI (T2W) mouse brain template to localize anatomically the PET signal in the ipsilateral and contralateral subventricular zone (SVZ) from the left to the right (b). The percentage of injected dose per cubic centimeter (%ID/cc; mean ± SD) of [^{18}F]FLT was quantified in the ipsilateral (c) and contralateral (d) SVZ. Sham *TLR4*$^{+/+}$ (n = 5), sham *TLR4*$^{-/-}$ (n = 5), MCAO *TLR4*$^{+/+}$ (n = 5), and MCAO *TLR4*$^{-/-}$ (n = 8) mice were examined by PET at two, seven, and 14 days after ischemia. *$p^{*} < 0.05$ compared with TLR4$^{+/+}$ and $p^{\&} < 0.05$ compared with control.*

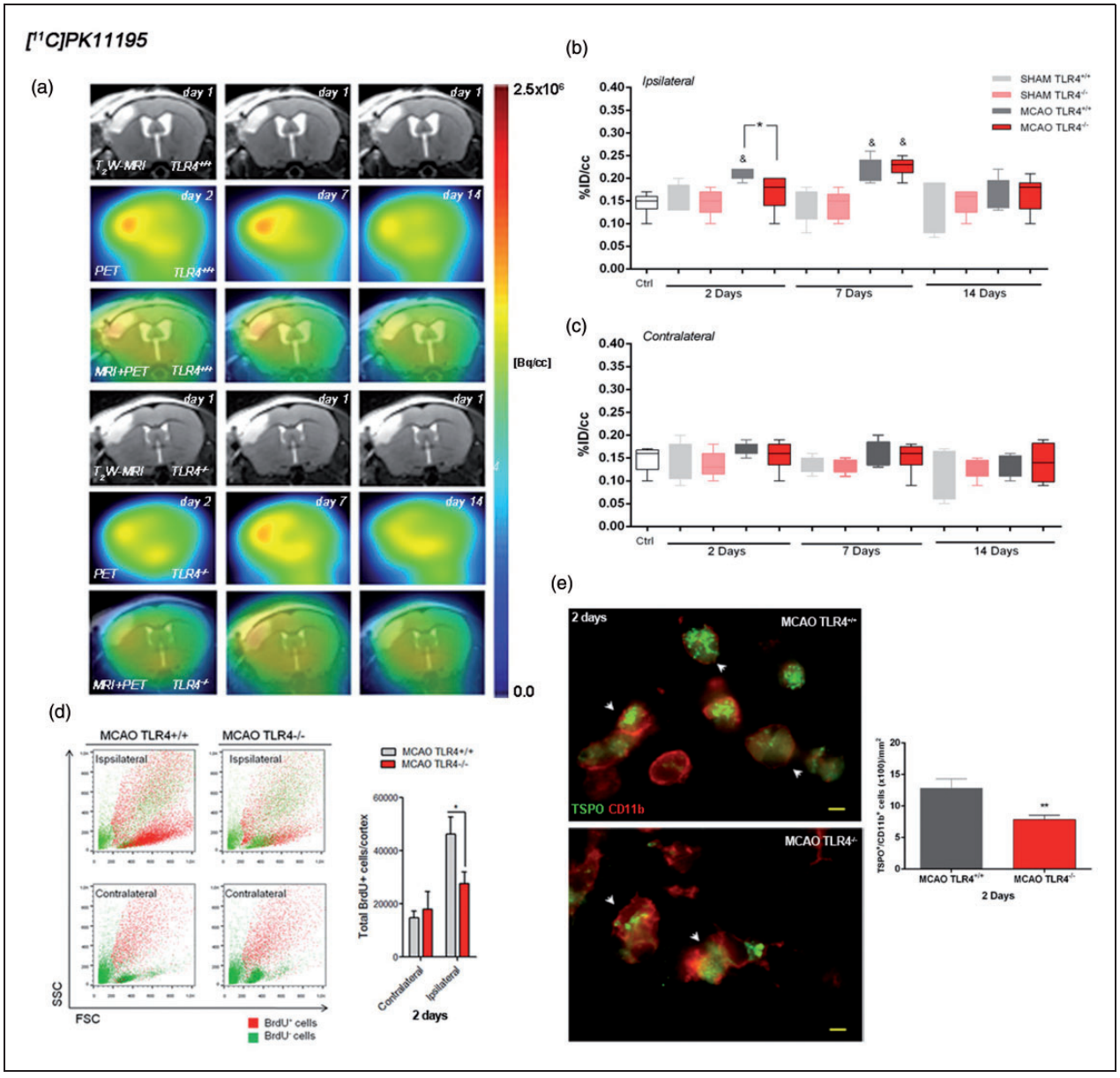

Figure 2. Role of TLR4 on microglia proliferation by using [^{11}C]PK11195 PET. MRI (T2-weighting (T2W)) at day 1 (upper row), positron emission tomography PET images of [^{11}C]PK11195 at two, seven, and 14 days after cerebral ischemia (middle row) and coregistered MRI-T_2WI and PET images (lower row) for TLR4$^{+/+}$ (upper panel) and TLR4$^{-/-}$ (lower panel) (a). Images correspond to the same representative animal for each time condition and radiotracer. The percentage of injected dose per cubic centimeter (%ID/cc; mean ± SD) of [^{11}C]PK11195 was quantified in the ipsilateral (b) and the contralateral (c) cortex. Flow cytometric analysis of new proliferative cells (total BrdU+ cells) in the ipsilateral and contralateral cortical area at two days after cerebral ischemia in mice that express TLR4 normally (gray column) (n = 5) and in TLR4-deficient mice (n = 4) (red column) (d). Immunofluorescence labeling of TSPO (green) and CD11b (red) and temporal profile of TSPO$^+$/CD11b$^+$ microglial cells (arrows) in the ischemic area at day 2 after MCAO in TLR4$^{+/+}$ (n = 3) and TLR4$^{-/-}$ (n = 4) (scale bars, 5 μm) (e). Sham *TLR4*$^{+/+}$ (n = 5), sham *TLR4*$^{-/-}$ (n = 5), MCAO *TLR4*$^{+/+}$ (n = 5), and MCAO *TLR4*$^{-/-}$ (n = 8) mice were examined by PET at two, seven, and 14 days after ischemia. $p^* < 0.05$ *and* $p^* < 0.001$ *compared with* *TLR4*$^{+/+}$, $p^{\&} < 0.05$ compared with control.

relation to TLR4 deficient mice (Figure 2(e); $p < 0.001$). Hence, these results support that the reduction of both [^{11}C]PK11195-PET signal and cell proliferation at day 2 in TLR4$^{-/-}$ mice was due to a decrease on microglial cells.

Discussion

Molecular imaging modalities have allowed the spatio-temporal evaluation of molecular events within the

diseased nervous system following stroke.[19] Despite this, the imaging of TLR4 effect on brain damage, inflammation,[4,5] and stroke-derived neurogenesis[15] following cerebral ischemia has been poorly evaluated to date. For this reason, we have explored the role of TLR4 on neurogenesis and inflammation after stroke in mice by using MRI and PET.

After cerebral ischemia, $TLR4^{-/-}$ mice have showed lower infarct volumes and better outcome in neurological evaluations.[15,16] Since differences in infarct volume may affect ischemia-induced responses, we performed a proximal occlusion of the MCA in TLR4-deficient mice and a distal occlusion of the MCA in wild-type animals ($TLR4^{+/+}$) to guarantee similar infarct volumes sizes in both mice groups (Figure 1(a)). In these conditions, our present data have shown the effect of TLR4 on both cell proliferation and neuroinflammation after cerebral ischemia.

[^{18}F]FLT binding evidenced a significant increase in the neurogenic activity at the ipsilateral SVZ of $TLR4^{-/-}$ mice at day 2 in comparison to $TLR4^{+/+}$ mice, followed by a progressive decrease over time (Figure 1(b) and (c)). These results are in agreement with the findings showing that TLR4 inhibits proliferation in the SVZ under physiological conditions[14] and those found by Moraga and collaborators where TLR4 exerted a negative effect on SVZ cell proliferation after stroke.[15] Likewise, PET studies showed a progressive nonsignificant trend toward an increase of [^{18}F]FLT binding in wild-type animals over time (Figure 1(c)). These results evidenced that the absence of TLR4 triggered an increase of proliferation in SVZ populations whereas in wild-type animals this increase was milder and delayed on time.

On the other hand, by using PET imaging and flow cytometry we have confirmed that ischemia—as reported—induced the microglia proliferation in the ipsilesional cortex when compared with the control group or contralateral hemisphere, respectively (Figure 2(b) and (d)). Importantly, TLR4 has been shown to be expressed in microglia and astrocytes after stroke and to be involved in neuroinflammation.[4,5] For instance, it has been recently shown that the inhibition of TLR4 with an antagonist protects against cerebral ischemia in mice by reducing the expression of inflammatory cytokines.[17] Likewise, it has been shown that 45% of the total number of BrdU positive cells in infarcted zone after stroke corresponds to reactive microglia[18] and that TSPO expression has also been attributed to the activation of microglia/infiltrated macrophages following cerebral ischemia.[2] Indeed, our results confirmed the TSPO expression in microglial cells in both $TRL4^{+/+}$ and $TLR4^{-/-}$ mice at day 2 after MCAO. In agreement with these findings, we observed a significant increase of [^{11}C]PK11195 binding, cortical BrdU positive cells, and microglia-expressing TSPO receptors in $TRL4^{+/+}$ mice in relation to $TLR4^{-/-}$ at day 2 after MCAO, evidencing the role of TRL4 on the neuroinflammation following cerebral ischemia.

In contrast, the protective effect of the lack of TLR4 on the inflammatory reaction was lost at day 7 after ischemia confirming that the effect of TLR4 on inflammation behaves in a time-dependent manner. Besides, the present study showed a relatively earlier TSPO overexpression in comparison to previous studies.[2,11,19,20] These differences may be related to differential pattern of leukocyte infiltration depending on the mice model of cerebral ischemia used.[21] According to this study, mice subjected to permanent MCAO showed both an earlier and extensive neuroinflammatory reaction than mice subjected to transient models of MCAO.

Summary and conclusions

In summary, we report here for the first time a PET imaging study of the effect of TLR4 on neurogenesis and inflammation following cerebral ischemia. These results show that the lack of TLR4 increases neurogenesis and inhibits acute inflammatory response after ischemia. Therefore, our data suggest that a more precise and personalized knowledge of inflammation and proliferation could foster the development of individualized treatments for the improvement of the outcome of these processes in different pathologies such as stroke.

Funding

The author(s) disclosed receipt of the following financial support for the research, authorship, and/or publication of this article: This work was supported by the Spanish Ministry of Economy and Competitiveness through grants SAF2012-33216 (Dr Moro), CSD2010-00045 (Dr Moro), SAF2015-52225-R (Dr Lizasoain), and SAF2014-54070-JIN (Dr Martín), by the Fondo Europeo de Desarrollo Regional RETICS RD12/0014/0003 (Dr Lizasoain), by the Regional Madrid Government S2010/BMD-2336 (Dr Moro), and S2010/BMD-2349 (Dr Lizasoain), and by the Department of Industry of the Basque Government for financial support.

Acknowledgements

The authors would like to thank M. González, A. Leukona, and M. Errasti for technical support in the radiosynthesis. Dr Cuartero was fellow of the Spanish Ministry of Economy and Competitiveness.

Declaration of conflicting interests

The author(s) declared no potential conflicts of interest with respect to the research, authorship, and/or publication of this article.

Authors' contributions

Substantial contributions to conception and design: AMo, JMP, JL, MH, MAM, AMa, IL. Acquisition of data: V G-V, MIC, BS, IM. Analysis and interpretation of data; AMo, ESS, AMa, IL. Drafting the article or revising it critically for important intellectual content: AMo, V G-V, MIC, BS, ESS, IM, JMP, JL, MAM, AMa, IL. Final approval of the version to be published: AMo, V G-V, MIC, BS, ESS, IM, JMP, JL, MAM, AMa, IL.

References

1. Rueger MA, Backes H, Walberer M, et al. Noninvasive imaging of endogenous neural stem cell mobilization in vivo using positron emission tomography. *J Neurosci* 2010; 30: 6454–6460.
2. Martin A, Boisgard R, Theze B, et al. Evaluation of the pbr/tspo radioligand [(18)f]dpa-714 in a rat model of focal cerebral ischemia. *J Cereb Blood Flow Metab* 2010; 30: 230–241.
3. Aderem A and Ulevitch RJ. Toll-like receptors in the induction of the innate immune response. *Nature* 2000; 406: 782–787.
4. Caso JR, Pradillo JM, Hurtado O, et al. Toll-like receptor 4 is involved in brain damage and inflammation after experimental stroke. *Circulation* 2007; 115: 1599–1608.
5. Caso JR, Pradillo JM, Hurtado O, et al. Toll-like receptor 4 is involved in subacute stress-induced neuroinflammation and in the worsening of experimental stroke. *Stroke* 2008; 39: 1314–1320.
6. Cao CX, Yang QW, Lv FL, et al. Reduced cerebral ischemia-reperfusion injury in toll-like receptor 4 deficient mice. *Biochem Biophys Res Commun* 2007; 353: 509–514.
7. Tang SC, Arumugam TV, Xu X, et al. Pivotal role for neuronal toll-like receptors in ischemic brain injury and functional deficits. *Proc Natl Acad Sci USA* 2007; 104: 13798–13803.
8. Aarum J, Sandberg K, Haeberlein SL, et al. Migration and differentiation of neural precursor cells can be directed by microglia. *Proc Natl Acad Sci USA* 2003; 100: 15983–15988.
9. Papadopoulos V, Baraldi M, Guilarte TR, et al. Translocator protein (18kda): new nomenclature for the peripheral-type benzodiazepine receptor based on its structure and molecular function. *Trends Pharmacol Sci* 2006; 27: 402–409.
10. Winkeler A, Boisgard R, Martin A, et al. Radioisotopic imaging of neuroinflammation. *J Nucl Med* 2010; 51: 1–4.
11. Rojas S, Martin A, Arranz MJ, et al. Imaging brain inflammation with [(11)c]pk11195 by pet and induction of the peripheral-type benzodiazepine receptor after transient focal ischemia in rats. *J Cereb Blood Flow Metab* 2007; 27: 1975–1986.
12. Schroeter M, Dennin MA, Walberer M, et al. Neuroinflammation extends brain tissue at risk to vital peri-infarct tissue: a double tracer [11c]pk11195- and [18f]fdg-pet study. *J Cereb Blood Flow Metab* 2009; 29: 1216–1225.
13. Gerhard A, Schwarz J, Myers R, et al. Evolution of microglial activation in patients after ischemic stroke: A [11c](r)-pk11195 pet study. *Neuroimage* 2005; 24: 591–595.
14. Rolls A, Shechter R, London A, et al. Toll-like receptors modulate adult hippocampal neurogenesis. *Nat Cell Biol* 2007; 9: 1081–1088.
15. Moraga A, Pradillo JM, Cuartero MI, et al. Toll-like receptor 4 modulates cell migration and cortical neurogenesis after focal cerebral ischemia. *FASEB J* 2014; 28: 4710–4718.
16. Hyakkoku K, Hamanaka J, Tsuruma K, et al. Toll-like receptor 4 (tlr4), but not tlr3 or tlr9, knock-out mice have neuroprotective effects against focal cerebral ischemia. *Neuroscience* 2010; 171: 258–267.
17. Hua F, Tang H, Wang J, et al. Tak-242, an antagonist for toll-like receptor 4, protects against acute cerebral ischemia/reperfusion injury in mice. *J Cereb Blood Flow Metab* 2015; 35: 536–542.
18. Popa-Wagner A, Badan I, Walker L, et al. Accelerated infarct development, cytogenesis and apoptosis following transient cerebral ischemia in aged rats. *Acta Neuropathol* 2007; 113: 277–293.
19. Zinnhardt B, Viel T, Wachsmuth L, et al. Multimodal imaging reveals temporal and spatial microglia and matrix metalloproteinase activity after experimental stroke. *J Cereb Blood Flow Metab* 2015; 35: 1711–1721.
20. Lartey FM, Ahn GO, Shen B, et al. PET Imaging of stroke-induced neuroinflammation in mice using [F]PBR06. *Mol Imaging Biol* 2014; 16: 109–117.
21. Zhou W, Liesz A, Bauer H, et al. Postischemic brain infiltration of leukocyte subpopulations differs among murine permanent and transient focal cerebral ischemia models. *Brain Pathol* 2013; 23: 34–44.